INTERFACIAL MIXING IN A DOUBLY-DIFFUSIVE FLOW IN THE PRESENCE OF SHEAR FLOW

by

Abdullah S. Al-Ghamdi[1] and Robert N. Meroney[2]

Submitted to

American Society of Mechanical Engineering
JOURNAL OF SOLAR ENERGY ENGINEERING

November 10, 1993 CEP93-94-ASAG-RNM-8

---

[1] Assistant Professor, Civil Engineering Department, King Abdulaziz University, p. o. box 9027, Jeddah 21413, Saudi Arabia.

[2] Professor and Director, Fluid Dynamics and Diffusion Lab., Colorado State University, Fort Collins, CO 80523, U. S. A.

KEY WORD LIST

BENTHIC BOUNDARY LAYER
DOUBLE-DIFFUSIVE CONVECTION
ENTRAINMENT
INTERFACIAL MIXING
INVERSIONS
LUTOCLINE
MIXING
SOLAR PONDS
STRATIFIED FLOWS
TURBULENCE

TABLE OF CONTENTS

INTERFACIAL MIXING IN A DOUBLY-DIFFUSIVE FLOW IN THE PRESENCE OF SHEAR FLOW

Abdullah S. Al-Ghamdi[2] and Robert N. Meroney[2]

ABSTRACT

An experimental investigation of the transient behavior of a doubly-diffusive flow under the influence of combined heating and shear flow is presented. The experimental work was performed in a relatively large salt tank (5 m long, 2 m deep and 1 m wide) with heat provided through the bottom wall and all the side walls of the tank were thermally and mass insulated. The fluid in the tank was initially layered into three distinctive layers: a bottom dense mixed layer, an upper light mixed layer and a linearly stratified layer in between. The shear was generated in the system by circulating the fluid of the upper layer through a pump and a heat exchanger to control the temperature of the moving layer. The temperature and density profiles as they evolved with time for various experiments are presented and discussed. The thickness of the interfacial layer is found to be inversely related to Richardson number, and the entrainment rate at the sharp interface between the layers was calculated and correlated to proposed scaling parameters.

1.0 INTRODUCTION

Double-diffusive phenomena occur in a fluid in which density is a function of two components of different molecular diffusivities (e.g., dissolved salt and heat). Based on the way the two driving gradients are oriented with respect to the gravitational field and the driving surface, double diffusion flows can be classified into three classes: 1) if both gradients are horizontal and perpendicular to the driving wall, a boundary layer flow along a vertical boundary results; 2) if a temperature gradient is horizontal and perpendicular to the driving wall (side heating problems) and the salt gradient is vertical and parallel to the driving wall, then a multicellular intrusive motion along the boundary will be induced; and finally, 3) if both gradients are vertical and perpendicular to the driving wall (bottom heating problems), the configuration resembles the Rayleigh-Benard stability problem, except that double-diffusive instabilities can develop even when the system is statically stable. Furthermore, the third class can be subdivided into two different modes depending on which of the components provides destabilizing force, namely the "salt fingering" mode and the "diffusive" mode. When the lower diffusivity component (e.g., salt) is destabilizing, the instability takes the form of long, thin convecting cells known as "salt fingers". On the other hand, the "diffusive" mode occurs when the higher diffusivity component (i.e., heat) is destabilizing; the he instability in this case is in the

[2] Assistant Professor, Civil Engineering Department, King Abdulaziz University, p. o. box 9027, Jeddah 21413, Saudi Arabia.

[2] Professor and Director, Fluid Dynamics and Diffusion Lab., Colorado State University, Fort Collins, CO 80523, U. S. A.

form of an overstable oscillation. The salt fingering mode is a subject by itself and will not be considered here; hence, the diffusive mode is the focus of this contribution.

Double-diffusive flows are a common feature of many natural and man-made systems. Examples of such flows in nature include the lifting of an atmospheric inversion layer due to the turbulent mixing at the tropopause, the deepening of the surface mixed layer in oceans into the stably stratified layer below owing to turbulence induced by surface wind or cooling, and the thickening of the sediment-suspension layer in the oceanic benthic boundary layer against the stratification of the lutocline. Such mixing processes are important in understanding and controlling the dispersion of pollutants in the environment.

In engineering applications such flows can be seen clearly in ocean discharge of Ocean Thermal Energy Conversion (OTEC) systems or power plants cooling water, aeration of drinking water and water-quality control in stratified reservoirs, disposal of waste water in reservoirs, heat storage in molten salt tanks, energy extraction from Salt Gradient Solar Ponds (SGSP), and storage and transport of liquid natural gas (LNG). In the chemical industry such flows can be observed during the processing of binary or multicomponent solutions of different diffusivities.

This study considered the transient behavior of temperature and salinity profiles as well as interfacial mixing at the upper interface for the system of fluid shown in Figure (1). As shown in the figure, the flow field consists of three layers: the bottom mixed layer at high salinity; the stably gradient layer in the middle; and the upper mixed layer at low salinity. The system is heated from below either by supplying a constant heat flux or by maintaining a constant temperature. The upper mixed layer is also maintained at a constant temperature by removing heat continuously. The upper layer undergoes a shear flow generated by discharge and suction diffusers placed above the interface. The system is completely insulated along the sides, and the temperature of the upper layer was chosen to match the ambient temperature to reduce heat loss to the surroundings. This flow configuration resembles the mixing in salty lakes and solar ponds.

2.0 PREVIOUS WORK

There is a considerable literature related to experiments devoted to stratified flows. The experiments undertaken are driven by either thermal mixing (heating only), mechanical mixing induced by grid generation (zero-shear) with (or without) heat, or the combination of both mean shear flow and heating. A comprehensive review of previous experimental work in each experimental category is given by Al-Ghamdi (1993).

A series of experiments were executed for density stratified flows subjected to mean shear or surface stress. The first experiment found in this category was completed by Kato and Phillips (1969), during which they applied a constant stress to the surface of an initially quiescent tank of fluid with uniform density gradient. The entrainment to the upper mixed layer which formed underneath the stress was found to be inversely related to the Richardson number based on the friction velocity and layer depth as: $E = u_e/u_* = 2.5\ Ri_{u*}$. Several years later, Kantha, Phillips and Azad (1977) extended the work of Kato and Phillips to a wider range of Richardson number

($30 < Ri < 1000$), but they found that no simple power law can represent the entrainment over the entire Richardson number range examined.

During an experiment performed by Narimousa and Fernando (1987), an upper mixed layer was moved over a dense layer by a disk pump. The results show that the thickness of the interfacial layer is much larger than the thickness of the thermal interfacial layer and both thicknesses are linear functions of the upper layer depth and are independent of the Richardson number. The entrainment was found to support an entrainment law of the form $E \sim Ri_u$.

Munoz (1986) and Munoz and Zangrando (1986) studied the mixing mechanism between a double-diffusive stratified layer and a mixed layer in the presence of bottom heating, a cross flow, and the combination of both. They performed experiments in a large salt-stratified tank with bottom heating and continuous withdrawal of fluid from one end of the bottom layer. They circulated fluid through an external heat exchanger and returned it to the opposite end at a lower temperature. Incropera, Lents and Viskanta (1986) completed a similar experiment in a smaller tank, and they found that under certain conditions the presence of shear flow attenuates the effect of buoyant mixing. The entrainment rate for this case is less than that for the bottom heating case.

Christodoulou (1986) combined data obtained for counter flows, buoyant flows, density currents, and surface stress experiments and showed that all the data could be represented on a common plot of the normalized entrainment rate as a function of the bulk Richardson number, using the interfacial velocity difference as the scale velocity. The correlation's exponent and constant are dependent on the Richardson number range: for low Richardson number the entrainment is constant (the Richardson number exponent is zero), and for high Richardson number the entrainment varies as the three halves power of Richardson number. It should be noted that in his analysis, Christodoulou neglected the molecular effects, even though it has been noted by other researchers that at high values of Richardson number the molecular effects are appreciable.

Johnstone and Zangrando (1988), and recently Fernando, Johnstone and Zangrando (1991) studied the effect of a turbulent jet on the mixing across the interface. The buoyancy of the exit jet was varied to obtain neutrally, positively, and negatively buoyant jets. The results from highly buoyant jets compare well with the results obtained from oscillating grids and vertical impinging jets. Negatively buoyant jet results compare well with recirculating channel results. Fernando (1991) and Al-Ghamdi (1993) provide reviews of turbulent mixing processes in stably stratified fluids.

3.0 EXPERIMENTAL SET-UP

The test tank used for this experiment is the same salt tank used by Munoz (1986), Munoz and Zangrando (1986), and Johnstone and Zangrando (1988). The tank has been relocated in the Hydraulics Laboratory at Colorado State University, and various improvements to the pumping system, instrumentation, and data-acquisition system were added. The test tank is a rectangular fiberglass cell approximately 1 m wide, 2 m deep, and 10 m long, which can be divided into two 5 m long sections. Only one section of this tank was used in the current study.

Heat is provided to the tank bottom by a number of heating strips spaced at 0.1 m intervals along the tank length and separated from the tank by a 2.5 mm steel sheet to ensure a uniform heat distribution over the bottom of the tank. During the constant temperature experiments, a CN9000 Omega temperature controller is used to regulate the heaters to maintain constant temperature in the bottom layer. The tank is insulated by covering its outside wall with 0.42 m solid polystyrene. Removable solid polystyrene plugs are used to insulate the windows when no flow visualization or velocity measurements are being taken.

Line discharge and suction diffusers were used to circulate the flow through a heat exchanger to remove the energy added by the pump and the energy extracted from the tank. The heat is removed by passing tap water through the heat exchanger. To control the jet buoyancy entering the tank, a CN-9000 Omega temperature controller is used to close or open a solenoid valve in PDI mode. Figure (2) shows the general schematic of the experiment and the position of instrumentation.

4.0 EXPERIMENTAL MEASUREMENTS

The data collected consists of flow rate, temperature, density, electrical power, and position. Measurements were fed to a data acquisition system (DAS). The DAS was used for data acquisition, reduction, storage, and equipment control.

In the initial experiments the flow rate was measured with an EFM turbine flowmeter and EFM-DC30 frequency-to-voltage converter. The EFM flowmeter has a linear calibration curve for flows between 2.5×10^{-4} and 2.0×10^{-3} m^3/s; the EFM has an uncertainty of 2% in this range. Later the EFM was replaced by a 1 inch orifice flowmeter calibrated in the Colorado State University's Hydraulic Laboratory calibration stand for flows between 2.94×10^{-4} m^3/s and $1.099 \times 10^{-3} m^3/s$.

From the calibration curve, the standard error of estimate (SEE) is found to be 8.65×10^{-6} m^3/s. The 95% confidence of interval uncertainty of the flow measurement can be taken as " 2(SEE) (Coleman, 1989); thus the maximum error occurs at minimum flow rate and is found to be "3%. During each experimental run the pump introduces a fluctuation in flow rate of "0.5%.

The fluid temperature at the discharge and suction diffusers, the ambient temperature in the laboratory, and the temperature distribution at the tank walls was measured by copper-constantan (Type T) thermocouples. The thermocouples signals were amplified by a Lawson Labs Model 20B thermocouples amplifier and fed to an IBM PC computer through a Lawson Labs Model 140 Analog Interface card. Lawson Labs PC64 data logging software was used as a data acquisition package. The thermocouples were calibrated and checked continuously, but no drift in measurements was noticed during the course of the current study. The Type T thermocouples has an uncertainty of " 1."C.

The temperature and density distribution in the middle of the tank was measured by a Model 125 Micro-Scale Conductivity Temperature Instrument (MSCTI) designed by Head (1983) to measure the temperature and electrical conductivity of water solutions containing ions. The MSCTI provides analog voltage outputs that are functions of the solution electrical conductivity and temperature. The probe was calibrated *in situ* according to the procedure outlined by Head (1983), and left emersed in the upper fresh water layer between measurements. It was checked continuously, and re-calibrated when deviation in measurements was observed. The error in density measurements is in the range of "0.5 kg/m^3. The MSCTI instrument was mounted on a motor driven platform. The platform was traversed upward in small, discrete intervals of 1 cm under control of the Fluke 1720 controller. Near the interfaces the intervals were reduced to 3 mm to obtain more data in the vicinity of the interface. At each location the platform remained for about one minute for temperature and density measurements, then moved to the next position. The position of the platform was determined by a precise potentiometer.

The amount of heat flux added to the system from the bottom was measured by continuous recording of electrical power averaged over the time span between scans. Due to the voltage fluctuation, the measured power yielded typical fluctuations of "10%. The amount of heat removed by the heat exchanger was calculated as the difference between the heat stored in the system and the heat added to the system, assuming that the conduction and radiation heat losses from the tank are negligible.

The diffuser heights were found by using meter scales submerged in the brine. The uncertainty in height measurements was " 0.002 m.The position of the interface was inferred from the density measurements.

5.0 EXPERIMENTAL PROCEDURE

To achieve an approximately linear gradient in the tank, a procedure suggested by Zangrando and Bertram (1985) was used. Once the required gradient conditions were determined, the tank was filled with tap water mixed with bulk food grade salt (NaCl) to a height that equals the thickness of the bottom mixed layer plus half of the total stratified layer. The salt and tap water were mixed thoroughly in a 50 gallon (0.19 m^3) fiberglass container placed at the top of the tank with a central drain plugged with a tightly fitted tube, then the well mixed brine is allowed to flow through the drain into the tank. To form the gradient layer a disk diffuser connected to a 38 mm PVC pipe was mounted on the traverse and connected through a hose to

tap water. The disk diffuser was placed approximately 50 mm above the desired position of the bottom of the stratified layer. The traverse was programmed to move the disk diffuser upward at a rate twice that of the rate of increase of water level in the tank. When the diffuser reached the surface of the water, the platform was stopped to mark the top of the stratified layer. The water continued to flow through the disk diffuser to form the upper fresh water layer. Finally, the water flow was terminated as the desired height of the upper layer was reached.

After the filling procedure was completed, the tank heaters were turned on to form temperature gradients. A linear gradient temperature was usually achieved in two to three days depending on the initial fluid temperature and the desired bottom temperature. Once the desired concentration and temperature gradients were achieved, the line diffusers were placed at a prescribed position above the upper interface and the pump was set to the required flow rate. For the same tank filling, a number of experiments might be performed by changing the flow rate and/or the heating conditions. A new filling was required when the thickness of the gradient layer became too small or when another salt stratification condition was desired. A total of eight experiments were performed to study the behavior of the entrainment in a double diffusive environment. In six experiments a constant temperature was maintained in the bottom layer, while in the remaining two a constant heat flux condition was imposed. In all experiments heat was removed from (or added to) the upper mixed layer by passing its fluid through an external heat exchanger to keep it at a constant temperature. The flow rate, initial salinity gradient, and diffuser position above the interface were varied to produce a wide range of mixing conditions. The experimental conditions used in this study are summarized in Table (1).

Each experiment ran for about 120 hours with data recorded every six to twelve hours; then a parameter was modified and another experiment started once the desired initial conditions were achieved.

Table (1): Experimental conditions.

Exp. Name	Flow rate (GPM)	Bottom Layer Temp.(deg.C) or Heat flux	Upper layer Temp.	$(dS/dH)_o^*$ (%/m)
MLL1	16	30	22	7.1
MHL2	16	196 W/m^2	22	8.5
HLL4	20.5	30	22	6
HHL5	20.5	196 W/m2	22	8.3
LLH8	11	32	22	9.15
MLH9	16	32	22	9.17
HHH10	20.5	42	22	13.5
MHH11	16	42	22	16.2

* $(dS/dH)o$ = The initial difference in salinity between bottom and upper mixed layers divided by the thickness of the gradient layer.

6.0 RESULTS AND DISCUSSION

6.1 Density and Temperature Distributions

The density and temperature profiles for experiment MLL1 are shown in Figures (3) and (4) respectively; they represent a typical behavior of the constant bottom temperature experiments. There are two sharp interfaces: one between the upper mixed layer and the gradient layer, and the other between the gradient layer and the bottom mixed layer. The two interfaces are expected to be independent. The gradient layer eroded from the bottom due to the convection velocity introduced by the bottom heating, and from the top due to both the presence of shear velocity generated by the flow and the convection velocity developed by heat extraction. It is evident that the erosion in the upper interface is greater than that in the lower one due to the presence of shear.

Figure (5) shows the density distribution of experiment MHL2 which features a constant heat flux of 196 W/m2 at the bottom. The density of the bottom layer increased initially because some salt deposited in the bottom of the tank was reintroduced into the fluid due to the convection generated by the heat in the bottom layer. The temperature distributions for the same experiment are shown in Figure (6). It can be seen from the temperature profiles that a boundary layer was formed near the bottom boundary which had a higher temperature than the bottom mixed layer. Unfortunately, due to experimental constraints, temperature measurements in the boundary layer were not possible.

The temperature profiles are illustrated here because they exhibit a very interesting phenomena. As the bottom mixed layer deepened with time, a second layer was seen to form above it; at a later time a third layer developed. This process continues until the whole stratified layer turned into a series of well mixed layers, as depicted in Figure (6). Turner (1965) experienced a similar behavior, and he argued that the first layer is the direct response to the applied heat flux, and that ahead of its advancing front a thermal boundary layer is produced by heat molecular diffusion. He also argued that both the temperature and the length scale of the thermal boundary layer increases with time until it eventually becomes unstable; then it breaks down and mixes to form a second layer.

Based on Turner's theory, Huppert & Linden (1979) predicted numerically and experimentally the average height of the layers. The average layer height (except the first layer) was approximated by:

$$h_{average} = 51\alpha^{1/2}(-g\beta_c\, dS/dz)^{-1/4} \qquad (1)$$

where: β_c the saline expansion, α is the thermal diffusivity, g is the gravitational acceleration, and (dS/dz) is the salinity gradient.

Equation (1) suggests that the vertical scale of the layers is independent of the heat flux and depends only on the initial salinity gradient. The average layer thickness using the above equations is 70.31 mm, while the actual value calculated from the temperature profiles was found to be about 61 mm. Kazmiercsak (1988) reported a layering in some of his experiments. He did not evaluate the average thickness of layers, but he reported that as time progressed merging of layers took place, and finally the entire system reduced into two layers. This result suggested that Equation (1) is only valid for certain period of time, but eventually the layering disappears.

The layering phenomena usually occurs when the stability number defined in Equation (2) exceeds a critical value:

$$R = Ra_T - \frac{Pr}{Pr+1} Ra_c \qquad (2)$$

where: R is the stability number, Pr is the Prandtl number, Ra_T and Ra_c are the thermal and solute Rayleigh numbers respectively. They are defined as:

$$Pr = \nu/\alpha_t, \qquad Ra_T = -\frac{\beta_t g \Delta T h^3}{(\alpha_t \nu)}$$
$$Ra_c = \frac{\beta_c g \Delta S h^3}{(\alpha_t \nu)} \qquad (3)$$

Turner (1974) found that the critical value of R is 24000, but Huppert and Linden (1979) claimed that their estimated value of $R_c = 10000$ is more accurate than Turner's value. They used the density profiles to determine the thickness of the first layer, while Turner estimated the layer thickness visually. It is clear from Equation (3) that a small error in the layer thickness will introduce a large error in the critical value of R. The R value calculated for experiment MHL2 is 1.06×10^{11}, which is several orders of magnitude higher than either suggested critical value.

6.2 Interface Progress

In the previous section typical temperature and density profiles were introduced, a reproduction of a sample density profile with an expanded vertical scale near the upper interface is shown in figure (7). By examining this figure, one can recognize three regions, namely the well mixed layer, the interfacial layer and the gradient layer. It was found that the interfacial layer has a thickness of 16-40 mm, and its slope is steeper than that of the gradient layer.

It is widely accepted that the thickness of the interfacial layer is the signature of the mixing process across the interface (E and Hopfinger (1988)), for weak stratification local instabilities can occur which thicken the interface. While for strong stratifications mixing is caused by the intermitted breaking of internal waves or due to the recoil of impinging eddies which results in a sharper interface. E and Hopfinger (1988) argued that for grid mixing

experiments, the interface thickness normalized by the distance between the source of turbulence (the grid) and the interface is a decreasing function of the Richardson number based on the shear velocity, with an asymptotic value at high values of the Richardson number. They suggested the following correlation:

$$\Delta h/d = 0.055 + 0.91 Ri^{-1} \qquad (4)$$

where: Δh is the interface thickness, d is the distance between the grid and the interface, and Ri is the Richardson number based on shear velocity. Following a similar analysis, Johnstone (1987) concluded that for impinging jet experiments, the interface thickness reaches a constant value of h/D= 0.05 for high values of Richardson numbers.

In Figure (8) the interfacial layer thickness normalized by the distance between the interface and the diffuser location is plotted against the Richardson number based on shear velocity along with Equation (4). The results are in good agreement with both E and Hopfinger and Johnstone results. The scattering of data was also noticed in previous workers results. The results suggest that the turbulent mixing process is similar regardless of the source of the turbulence.

To define the height of the interface, the data in the interfacial layer were fitted to an analytic curve through regression, and the intersection of this curve with the upper layer marked the location of the interface. Similarly, the thickness of the interfacial layer was determined as the distance from the point of intersection of the curve-fitted interfacial layer data and gradient layer data to the location of the interface.

Thus, the density step across the interfacial layer, which is used in the definition of the Richardson number, is defined as:

$$\Delta\rho = \frac{d\rho}{dz}\Big|_{interface} \Delta h \qquad (5)$$

where: Δh and $d\rho/dz$ are the thickness and the slope of the interfacial layer, respectively.

The uncertainty in the density jump across the interface can be found from the correlation:

$$\left(\frac{U_{\Delta\rho}}{\Delta\rho}\right)^2 = \left(\frac{U_{d\rho/dz}}{d\rho/dz}\right)^2 + \left(\frac{U_{\Delta h}}{\Delta h}\right)^2 \qquad (6)$$

From the linear fitting of the density profile across the interface the typical uncertainty in the slope was found to be "4%. The interface thickness has uncertainty of "9%, and by using equation (6) the calculated uncertainty in density jump across the interface is "10%.

The height of the interface as it progresses with time for experiment HHH10 is shown in Figure (9). The data for interface progression in all experiments are fitted with second order polynomials to facilitate the calculation of the entrainment velocities.

To prepare a qualitative comparison between the different experiments, the upper interface locations for all the experiments non-dimensionalized by the initial interface height are plotted in Figures (10) and (11). Figure (10) indicates that the maximum entrainment occurs in experiment HLL4, which has a high flow rate and low temperature and salinity gradients. By comparing various curves in Figures (10) and (11) one can determine that the higher the shear flow, the more entrainment occurs. On the other hand the presence of temperature and salinity gradients slows the entrainment rate. These results confirm that the entrainment rate may be inversely related to Richardson number based on shear velocity and density gradient. The entrainment velocity, U_e, the rate at which the upper interface is moving downward, is obtained by differentiating the second order equations representing the interface position with respect to time.

6.3 Extracted Energy

To calculate the convective velocity in the upper layer, one should know the amount of heat added/removed from this layer. The amount of energy extracted from the system to keep the upper mixed layer temperature constant is calculated from the temperature profiles. The procedure followed for the constant heat flux experiments is slightly different from that used with constant temperature experiments. These procedures are described in the following sections:

6.3.1 Constant Heat Flux Experiments

For the constant bottom heating experiments, the energy removed is simply the difference between the energy provided to the system through the bottom of the tank and the energy stored in the brine, based on the assumption that the system is well insulated and the energy loss is minimal. The energy stored in the brine at any time is related to the integration of the temperature profile at that time and the temperature profile at the beginning of the experiment (t=0) according to the correlation:

$$E - E_o = \rho C_p A \int_0^{z_u} [T(z,t) - T(z,t_o)]\, dz \qquad (7)$$

where: E_o is the energy in the system at initial time (KJ), E is the energy in the system at time t, (KJ), T(z,to) is the temperature profile at initial time, T(z,t) is the temperature profile at time t, ρ is the fluid density (kg/m^3), C_p is the specific heat,($KJ/kg^\circ C$), z_u is the height of water in the tank, and A is the tank cross-sectional area.

The amount of heat extracted from the system can readily be obtained from the energy balance of the system. Thus:

$$\rho C_p A \frac{d(E-E_o)}{dt} = Q_{H_i} - Q_{H_o} \qquad (8)$$

where: Q_{Hi} is the heat added to the bottom layer, and Q_{Ho} is the heat removed from the upper layer.

6.3.2 Constant Temperature Experiments

For the constant bottom temperature experiments, the amount of energy removed from the system can be calculated from the temperature profile using the following correlation:

$$E_o - E = \rho C_p A \int_{z_1}^{z_u} ((T(z, t_0) - T(z, t)) \, dz \qquad (9)$$

where: z_1 is the point of intersection of the temperature profile at initial time (i.e t=0) and the temperature profile at time t, (see Figure (12)), and the rest of variables are as previously defined. The amount of heat removed is then calculated by differentiating Equation (5) with respect to time. Thus; in Figure (15):

$$Q_{H_o} = \rho C_p A \frac{d(E-E_o)}{dt} . \qquad (10)$$

As an illustrating example the energy removed from the system for experiment LLH8 is shown

6.4 Entrainment Correlations

In Section 6.2, the entrainment of the fluid into the upper mixed layer was discussed. As we have seen in Figures (10) through (11), there is a distinctive entrainment curve for each single experiment. It would be very helpful from the engineering practical point of view if one could collapse all the entrainment curves to a single meaningful curve. This correlation may be obtained through a dimensional analysis procedure. The important variables in the problem are illustrated schematically in Figure (13).

Assuming that the molecular properties such as viscosity and thermal and solute diffusivities have a negligible effect on the phenomenon of turbulent mixing, then we have:

$$U_e = \phi(H, \Delta h, U, \rho, \Delta\rho, g) . \qquad (11)$$

By performing a standard pi-theory dimensional analysis, one obtains:

$$\frac{U_e}{U} = F\left(\frac{\Delta h}{H}, \frac{\Delta \rho}{\rho}, \frac{U^2}{gH}\right). \qquad (12)$$

The last two terms in equation (12) can be combined into a single dimensionless number, i.e., the overall Richardson number defined as:

$$Ri_o = \frac{g\Delta\rho H}{\rho U^2} = \frac{g'H}{U^2}, \qquad (13)$$

where the density jump across the interface is obtained from the correlation:

$$\Delta\rho = \Delta h \frac{\partial \rho}{\partial z}. \qquad (14)$$

It is safe to assume that normally the interfacial layer thickness is much smaller than the upper mixed layer thickness, and equation (12) reduces to:

$$\frac{U_e}{U} = f(Ri_o). \qquad (15)$$

Entrainment correlations of the form represented above have indeed been suggested by many workers, unfortunately, it is the choice of the right length scale (H) and velocity scale (U) that makes the correlation meaningful. In some experimental configurations, this choice is obvious, but in experiments involving jet-generated shear, like the one considered in this study, the choice of scaling velocity and length is not straightforward. So several formulations of Richardson numbers were examined in this study.

It seems appropriate to take the distance between the neutrally buoyant jet centerline and the interface location, d, as the scaling length. This distance represents the distance between the source of turbulence and the interface, logically it is clear that the closer the source of turbulence to the interface, the higher the entrainment should be.

One may next consider some five alternative velocity scales for the system, and then select the one (or the combination of more than one) that provides the best entrainment correlation :

1. The jet enters the tank with an inlet velocity, u_o. Knowing the flow rate of the jet, this velocity is simply:

$$u_o = \frac{Q}{A_o}, \tag{16}$$

where: Q is the flow rate and A_o is the diffuser area.

2. The bulk flow velocity can be calculated by equating the horizontal momentum flux at the point where the jet edge intersects the interface to the inlet momentum flux. Assuming a top-hat velocity profile, the bulk flow velocity is defined as:

$$u = \left(\frac{M_o}{wd}\right)^{\frac{1}{2}}, \tag{17}$$

where: M_o is the jet exit momentum flux, w is the width of the tank, and d is the distance between the jet axis and the interface.

3. For a neutrally buoyant jet, the centerline velocity is related to the jet exit velocity by (Johnstone and Zangrando 1988):

$$\frac{u_c}{u_o} = 2.28\frac{B}{x_i}, \tag{18}$$

where B is the diffuser slot height, and $x_i = d/0.14$ is the horizontal distance to the impingement point.

4. Munoz and Zangrando (1986) argued by dimensional reasoning that the an effective shear velocity can be defined as:

$$u_* = \frac{\sqrt{M_o}}{d}. \tag{19}$$

5. Since the system involved heating (or cooling) of the upper layer, natural convection occurred in the layer, and the convective velocity generated by heat must be represented in the scaling velocity. Following Bergman et al. (1983), the convective velocity is defined as:

$$w_* = \left(\frac{g\beta_t Q_H H}{\rho C_v}\right)^{1/3}, \tag{20}$$

where: β_T is the coefficient of thermal expansion, Q_H is the applied heat flux (kw/m^2), C_v is the specific heat (KJ/kg/C), ρ is the average density of the layer, and H is the thickness of the layer.

The entrainment correlation based on the bulk flow velocity, u as the scaling velocity showed large scatter, suggesting that the bulk flow velocity by itself does not completely characterize the flow mixing. Similar correlations were developed using u_o, u_*, and u_c as scaling velocity, and the results were not encouraging. Also, when the convective velocity, w_*, was used as the scaling velocity, the scatter was rather large. An alternative approach would be to propose a velocity scale resulting from combination of characteristic velocities.

1. A weighing formulation of the form represented in Equation (21) is suggested by Munoz and Zangrando (1986):

$$U_* = [(cu_*)^3 + w_*^3]^{1/3} \qquad (21)$$

Using u instead of u_* in Equation (21), and the weighing coefficient c = 0.15, the entrainment correlation is plotted in Figure (14).

2. One might consider using a linear combination of two different Richardson numbers in the ordinate, one based on u and the other based on w_*. Using the following formulation:

$$Entrainment = U_e/U_*, \qquad Ri = 100Ri_u + Ri_{w_*} \qquad (22)$$

the data are plotted in Figure (15). This approach provides the best correlation between the data, and it approaches the anticipated asymptotic value at high values of Richardson number.

7.0 VIRTUAL CORRELATIONS

Dimensional analysis is a powerful tool used very frequently in fluid mechanics and related areas, but great care should be taken in utilizing the concept of dimensional analysis because sometimes the results may be misleading. It is a widely accepted practice to present experimental or field data on a single dimensionless plot of one dimensionless group correlated against another. If a common variable is used as a scaling quantity in both the abscissa and ordinate, then an artificial correlation may be introduced between the two dimensionless quantities which contributes to correlation between the dimensionless parameters even though they may be totally independent (Hicks,1978; Meroney, 1986; and El-Badry, 1993).

Hicks (1978) pointed out that if two variables: $y = x_1 x_2^{\ a}$ and $z = x_3\ x_2^{\ b}$ are plotted in a log-log plot, then the artificial correlation between y and z can be calculated from the expression:

$$r = \frac{ab\Delta x_2^2}{[(\Delta x_1^2 + a^2\Delta x_2^2)(\Delta x_3^2 + b^2\Delta x_2^2)]^{1/2}} \qquad (23)$$

where Δx_i represents the error in x_i value.

In Section (6.4) different correlations between the entrainment and the Richardson number were introduced. A common scale velocity is used in both the definition of dimensionless entrainment velocity ($E = U_e/U_*$) and in the Richardson number ($Ri = g\Delta\rho d/\rho/U_*^2$). In this section the virtual correlation between E and Ri introduced by using this common scale velocity is examined. The Richardson number can be written as ; $Ri = UU_*^{-2}$, where $U = g\Delta\rho d/\rho$ and the error in U calculated from Equation (24) is 11%. Using Equation (4.22) to find the artificial correlation, yields:

$$r = \frac{(-1)(-2)(.06^2)}{[(.20^2+1^2(.06)^2)(.11^2+4(.06)^2)]^{1/2}} = 0.21$$

this correlation value is small and suggests that the virtual correlation introduced by the dimensionless grouping is not dominant, since the correlation of the actual data was r = 0.87.

8.0 CONCLUSION

The phenomenon of double diffusive flow, where both heat and concentration coexist in the flow field, was investigated in this research. The experimental work was performed in a 1 m wide by 2 m deep by 5 m long thermally stratified salt tank. Initially the system consisted of three different layers; a bottom mixed layer, a middle linearly and stable stratified layer, and an upper mixed layer. The bottom wall was heated either at a constant heat flux or at a constant temperature, the upper boundary was a free surface, while the remaining walls were completely insulated. The upper mixed layer was subjected to shear flow.

This study provides an understanding of the development of temperature and density profiles in such systems, which are analogs to the mixing processes found in solar ponds and lakes. The measurements led to considerable insight about the mixing process at a sharp interface undergoing both heating and shear flow, and the results permit the following conclusions:

1. A middle gradient layer will erode from the bottom due to convective mixing introduced by the bottom heating, and it will erode from the top due to the presence of both a shear velocity convective velocities generated by heat extraction.

2. For constant bottom temperature conditions, the entrainment at the lower interface will be low, the thickening of the bottom layer will be very slow, and the layer will approach steady state for most conditions. But for constant heat flux situations the entrainment at the bottom mixed layer will be rapid.

3. An interfacial layer will form between the gradient and mixed layers. The thickness of this layer was found to be in the range of 16 mm to 40 mm for all the experiments. This layer thickness was found to be related to Richardson number, and it seemed to reach a constant value at high values of Richardson number.

4. In some cases during constant bottom heat flux conditions, a layering phenomena occurs during which the entire tank depth will be occupied by a series of well mixed layers. The average thickness of these layers was found to be 61 mm. The layering phenomena is expected to occur only if the stability number exceeds a critical value of the parameter R, but a unique value for this parameter has not be determined.

5. The entrainment rate is dependent on both the convective and shear velocities. A good correlation was found to have the form: $U_e/U_* = a(100Ri_u + Ri_{w*})^b$.

The understanding of the phenomenon of double diffusive mixing is far from complete, and there is a need for further work which may include measurements that were not possible during the conduct of this research. Further insight into the problem would be achieved by expanding the flow measurement technique to include the velocity distribution as well as the velocity fluctuations. Measurement of low velocities in salty systems is not an easy task, but with the latest developments in Laser Doppler Velocimetry (LDV) and Particle Image Velocimetry (PIV) such measurement are possible. Also refined measurement of temperature, salinity and velocity in different locations and in different directions would allow for determination of whether such systems exhibit 1-D, 2-D, or fully 3-D flow features. Finally using a suitable flow visualization technique would help identify the regions of turbulent flow and may lead to better understanding of the mixing process.

NOTATION

Symbol	Definition
A	Tank cross-sectional area
A_o	Diffuser area
C_p	Thermal capacity
d	Diffuser height above the interface
D	Mass molecular diffusivity
g	Gravitational constant
H	Upper interface height
M_o	Jet exit momentum flux
p	Pressure
Pr	Prandtl number (ν/α)
Q	Flow rate
Q_H	Heat flux
R	Stability number
Ra_c	Conc. Rayleigh number ($g\alpha\Delta Th^3$) / ($k\nu$)
Ra_t	Temp. Rayleigh number ($g\alpha\Delta Ch^3$) / ($k\nu$)
Re	Reynolds number (u_{max} H/ν)
Ri	Bulk Richardson number ($g\ \Delta\rho_{max}\ H$)/($\rho\ U^2$)
t	Time
T	Temperature

U	Scale velocity
u_c	Jet centerline velocity
u_*	Jet shear velocity
U_*	Combined shear velocity = $f(u_* + w_*)$
U_e	Entrainment velocity
w_*	Convective velocity
z_u	Water surface position

Greek Symbols

α	Thermal molecular diffusivity
β_T	Thermal expansion coefficient
β_C	Saline expansion coefficient
Δh	Interfacial layer thickness
ρ	Density

REFERENCES

Al-Ghamdi, A. S., (1993), Experimental and Numerical Study of a Doubly-Diffusive Flow Subjected to Combined Heating and Shear, Ph. D. Dissertation, Civil Engineering Department, Colorado State University, Fort Collins, CO.

Bergman, T. L. , F. P. Incropera, and R. Viskanta, (1986), "Correlations of Mixed Layer Growth in a Double-Diffusive, Salt Stratified System Heated From Blew," ASME Journal of Heat Transfer, Vol. 108, pp. 206-211.

Christodoulou, G. C., (1986), "Interfacial Mixing in Stratified Flows," Journal of Hydraulic Research, Vol. 24, No. 2, pp. 77-87.

Coleman, H. W., and W. G. Steele,(1989), Experimentation and Uncertainty Analysis for Engineers, John Wiley & Sons, Inc., New York.

E, Xuequan, and E. J. Hopfinger, (1988), "On Mixing Across an Interface in Stably Stratified Fluid," J. Fluid Mechanics, Vol. 166, pp. 227-244.

El-Badry, H., (1993), " " Ph.D. Dissertation, Civil Engineering Department, Colorado State University, Fort Collins, CO.

Fernando, H. J., (1991), "Turbulent Mixing in a Stratified Fluids," Annual Rev. Fluid Mech., Vol. 23, pp. 455-493.

Fernando, H. J., H. Johnstone, and F. Zangrando, (1991), "Interfacial Mixing Caused by Turbulent Buoyant Jets," Journal of Hydraulic Engineering, Vol. 117, pp. 1-19.

Head, M. J., (1983), The use of Miniature Four-Electrode Conductivity Probes for the Measurements of Turbulent Density or Temperature Variation in Salt-Stratified Water Flows, Ph.D. Dissertation, University of California, San Diego, CA.

Hicks, B. B., (1978), "Some Limitations of Dimensional Analysis and Power Laws," Boundary Layer Meteorology, Vol. 4, pp. 567-569.

Huppert, H. E., and P. F. Linden, (1979), "On Heating a Stable Salinity Gradient From Below," J. Fluid Mechanics, Vol. 95, part 3, pp. 431-464.

Incropera, F. P., C. E. Lents, and R. Viskanta, (1986), "Gradient Layer Entrainment in a Thermohaline System With Mixed Layer Circulation," J. of Solar Energy Engineering, Vol. 108, pp. 267-274.

Johnstone, H. W. , and F. Zangrando, (1988), "Mixing Depth of a Submerged, Horizontally Injected Buoyant Jet," J. of Solar Energy Engineering, Vol. 110, pp. 125-131.

Kantha, L.H., O.M. Phillips, and R.S. Azad, (1977), "On Turbulent Entrainment at a Stable Density Interface," J. of Fluid Mechanics, Vol. 79, pp. 753-768.

Kazmierczak, M. J., (1988), Transient Double Diffusion in a Fluid Layer and a Composite Porous/Fluid Layer Heated From Below, Ph. D. Dissertation, University of Illinois at Chicago.

Kato, H., and O. M. Phillips, (1969), " On the Penetration of a Turbulent Layer Into Stratified Fluid," J. of Fluid Mechanics , Vol. 34, Part 4, pp. 643-655.

Meroney, R.N., (1986), "Apparent Correlation of Data Produced by Using Correlated Variables in Ordinate and Abscissa Parameters," Colorado State University, Report No. CEM86-87RNM48, Appendix A, 9 pp.

Munoz, D. R., (1986), Investigation of Entrainment in a Double-Diffusive Thermohaline System with Mixing Driven by Bottom Heating and Horizontal Recirculation, Ph.D. Dissertation, Purdue University, Lafayette, Indiana.

Munoz, D., and F. Zangrando, (1986), Mixing in a Double-Diffusive, Partially Stratified Fluid, SERI, Report No. TR-252-2942.

Narimousa, S., and H. J. Fernando, (1987), "On the Sheared Density Interface of an Entraining Stratified Fluid," J. Fluid Mechanics, Vol. 174, pp. 1-22.

Turner, J. S., (1965), "The Coupled Turbulent Transports of Salt and Heat across a Sharp Density Interface," Intl. J. Heat and Mass Transfer, Vol. 8, pp. 759-767.

Turner, J. S., (1974), "Double-Diffusive Phenomena", Ann. Rev. Fluid Mech., Vol. 6, pp. 37-56.

Zangrando, F., and L. Bertram, (1985), "The Effect of Variable Stratification on Linear Double-Diffusive Stability," J. Fluid Mech., Vol. 151, pp. 55-79.

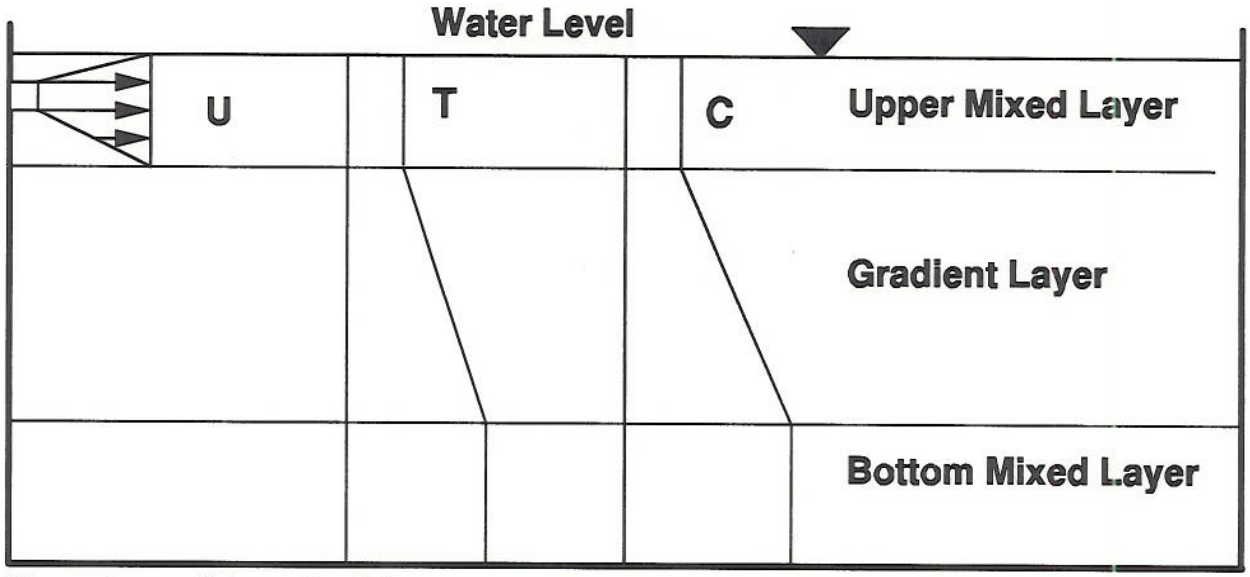

Figure 1 Schematic of the system

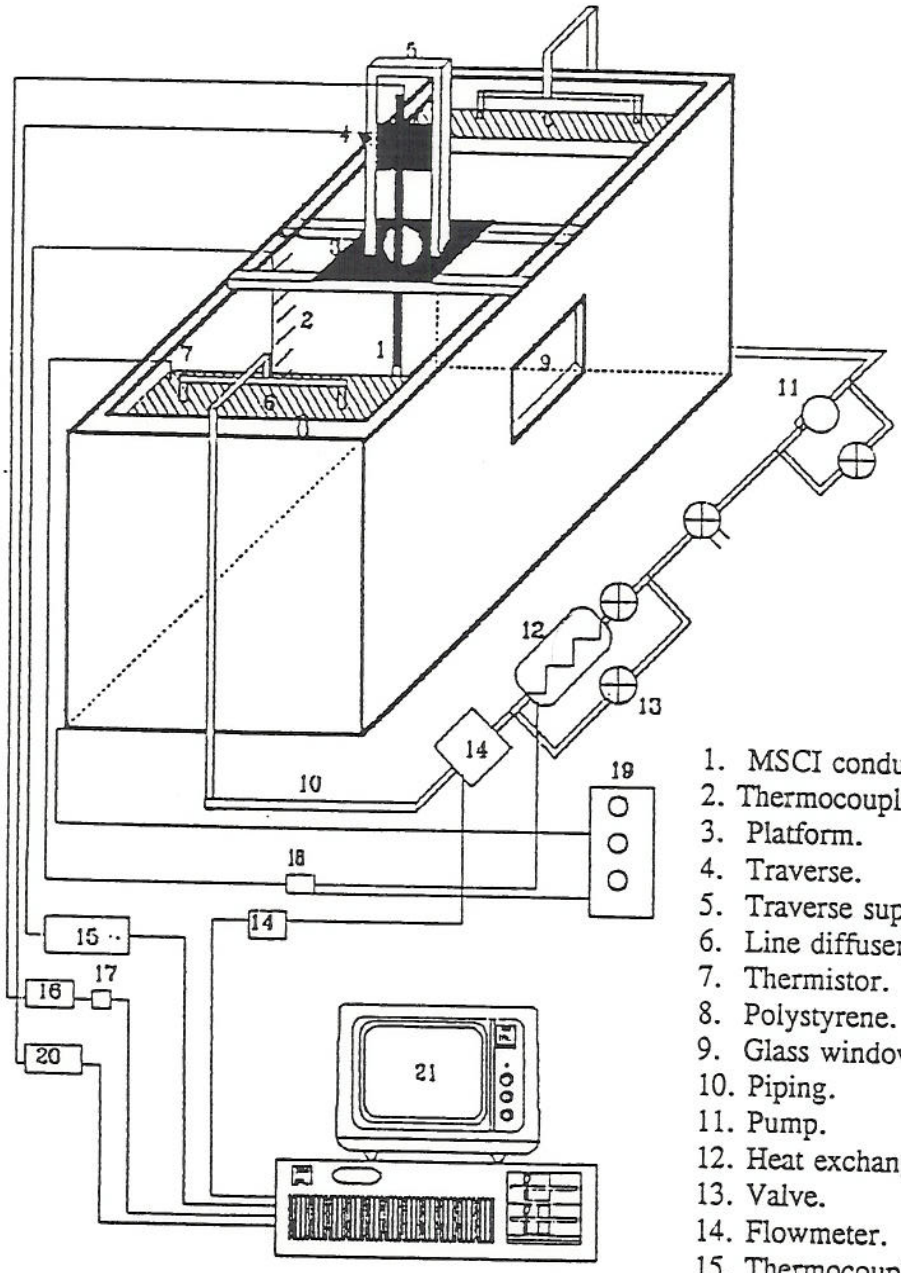

Figure 2 Experimental Layout

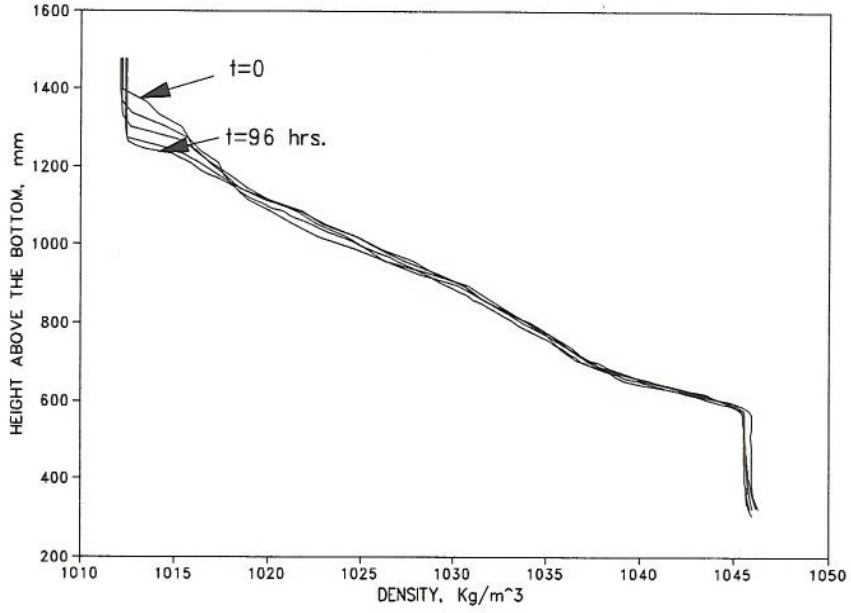

Figure 3 Density Distribution for Experiment MLL1

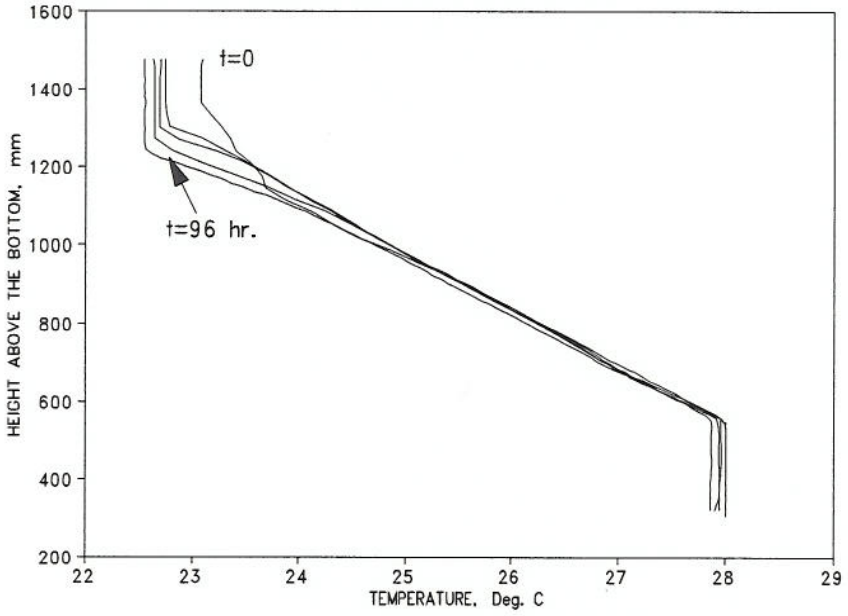

Figure 4 Temperature Distribution for Experiment MLL1

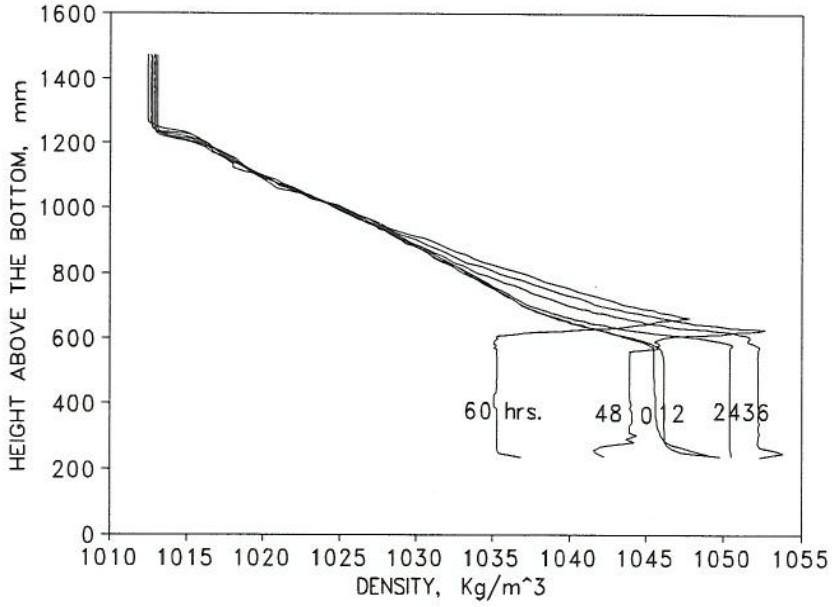

Figure 5a Density Profiles for Experiment MHL2

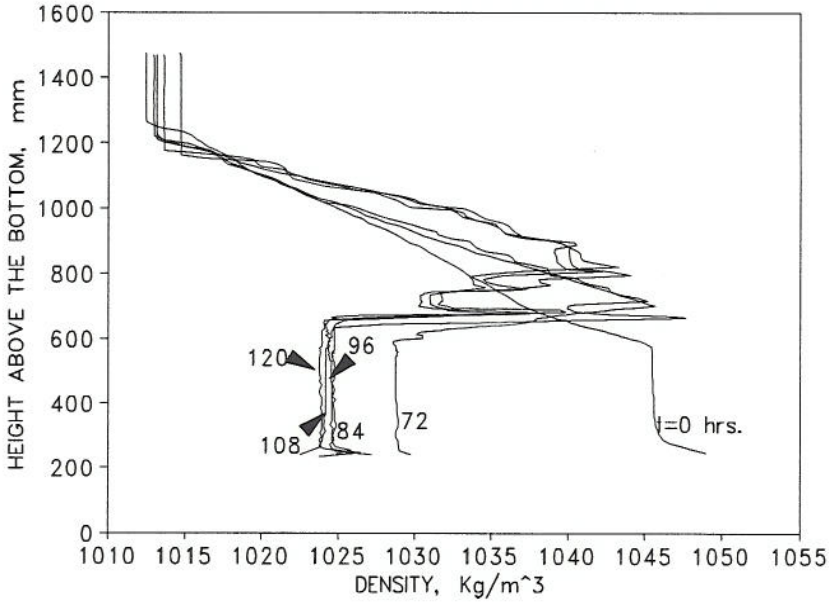

Figure 5b Density profiles for Experiment MHL2 (Continued)

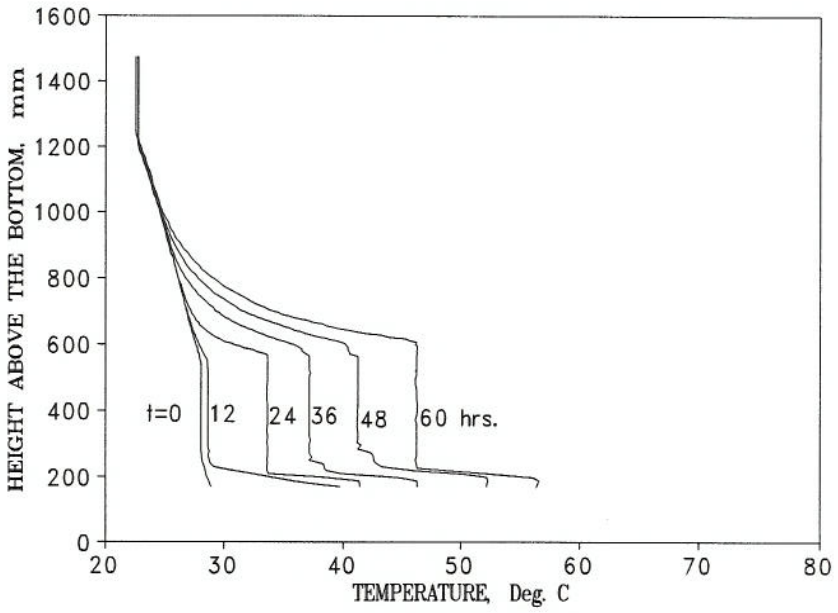

Figure 6a Temperature Profiles for Experiment MHL2

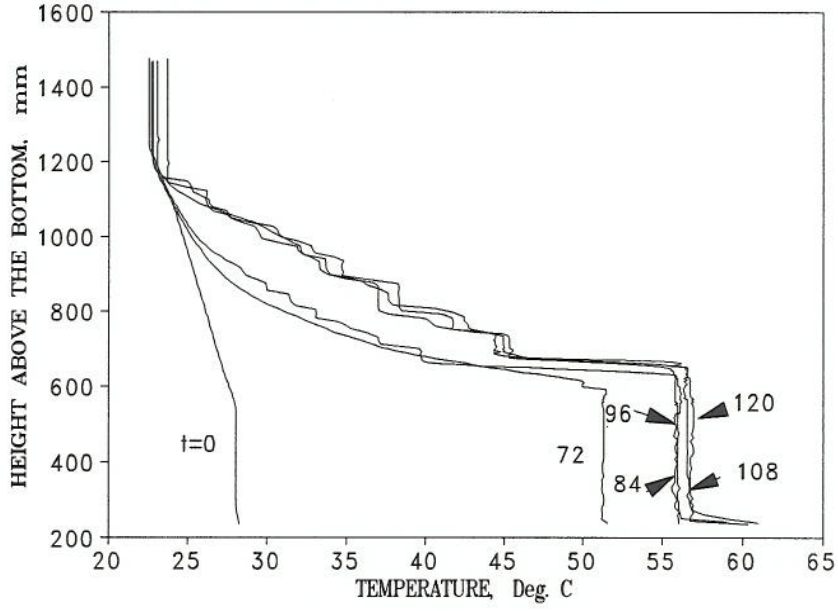

Figure 6b Temperature Profiles for Experiment MHL2 (Continued)

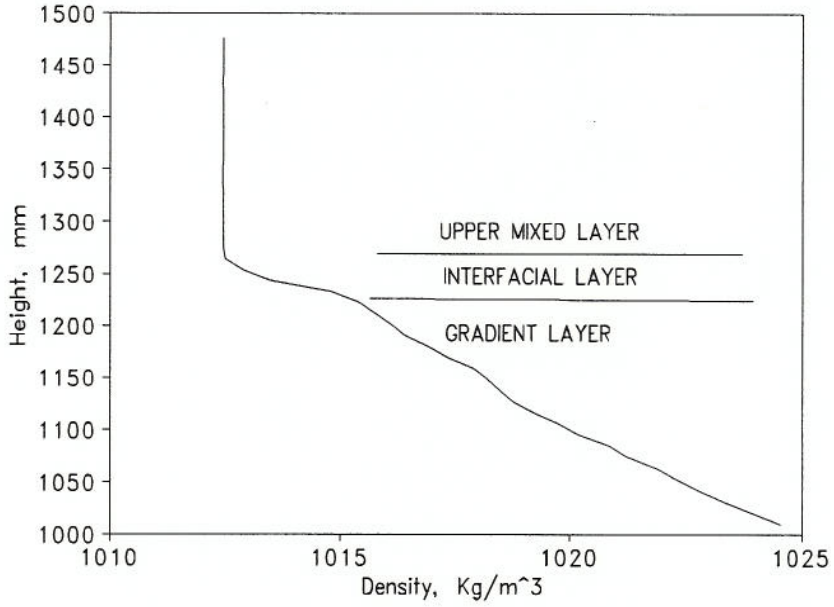

Figure 7 Density Profiles Near the Upper Interface

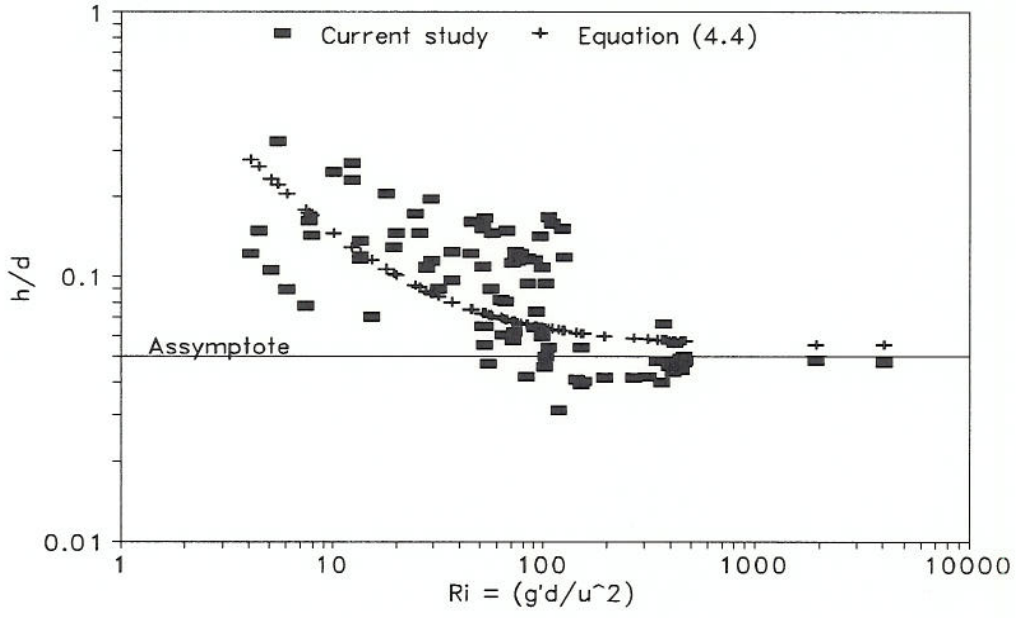

Figure 8 Interfacial Layer Thickness

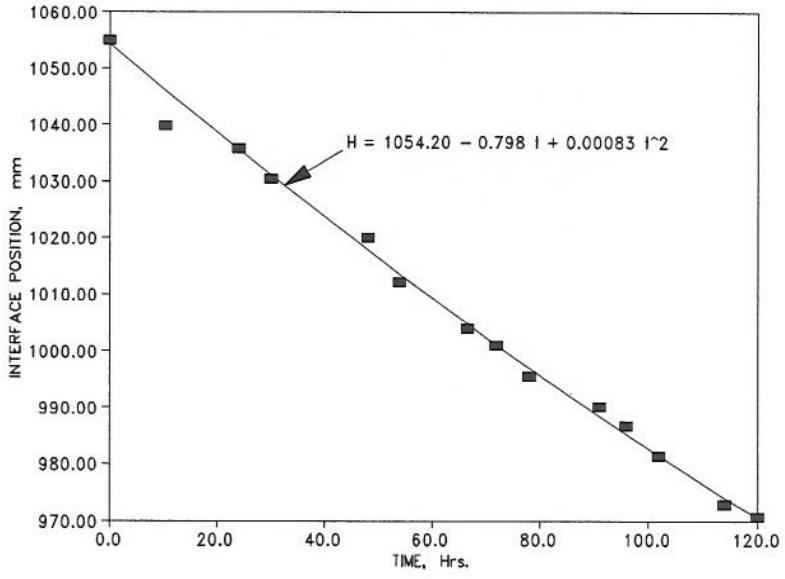

Figure 9 Interface Locations for Experiment HHH10

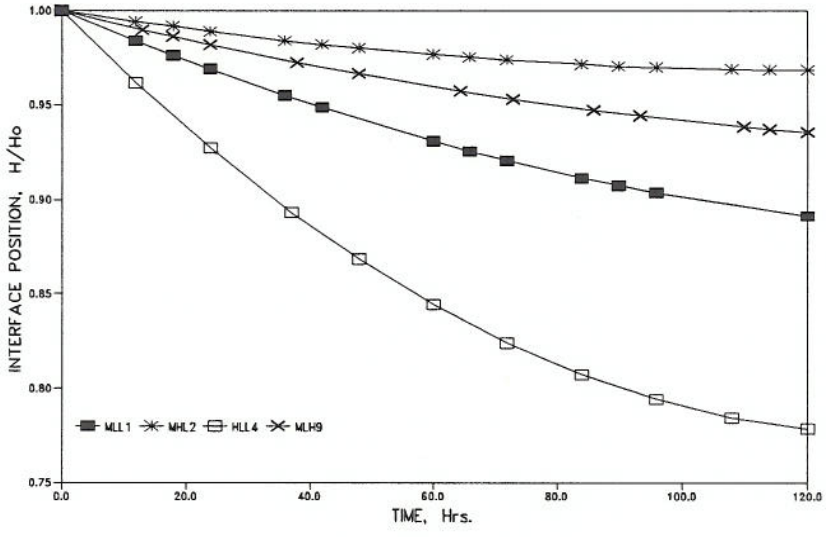

Figure 10 Dimensionaless Interface Height Experiments MHL2, MLH9, MLL1, and HLL4

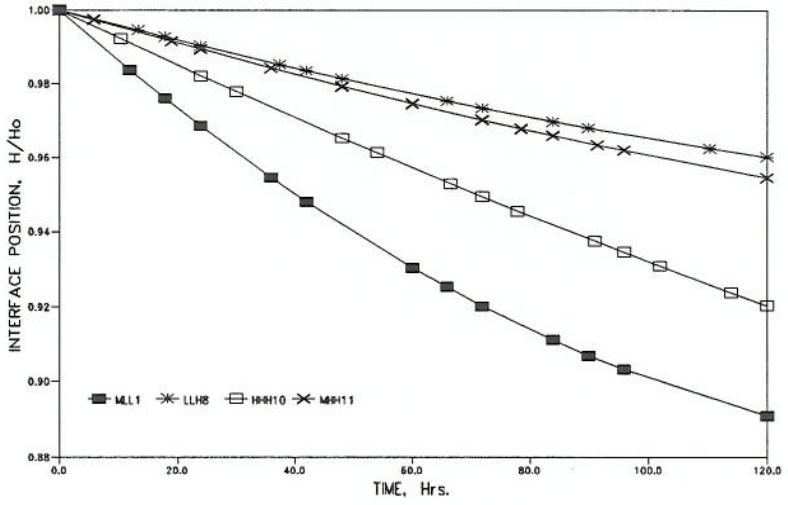

Figure 11 Dimensionless Interface Height for Experiments LLH8, MHH11, HHH10, and MLL1

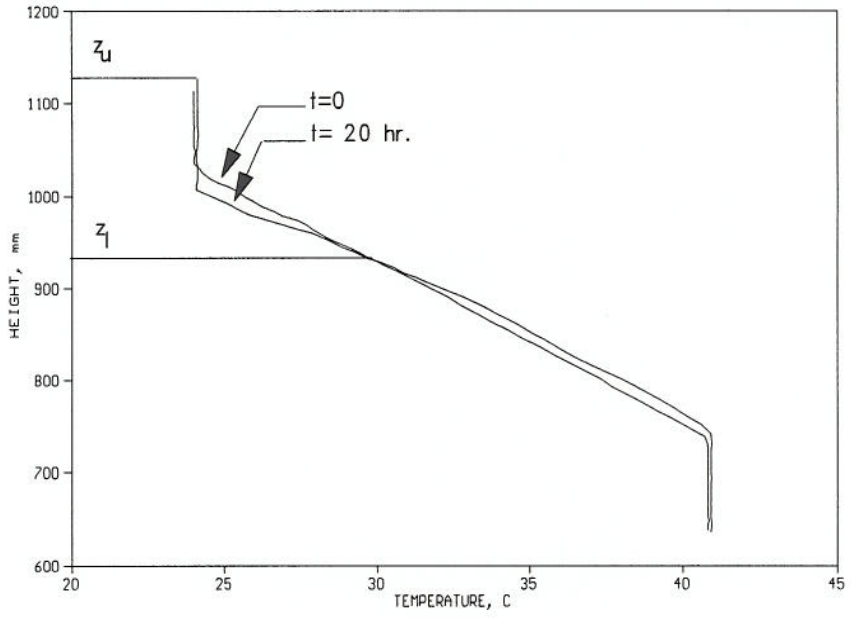

Figure 12 Typical Heat Flux Calculations for Constant Temperature Experiments

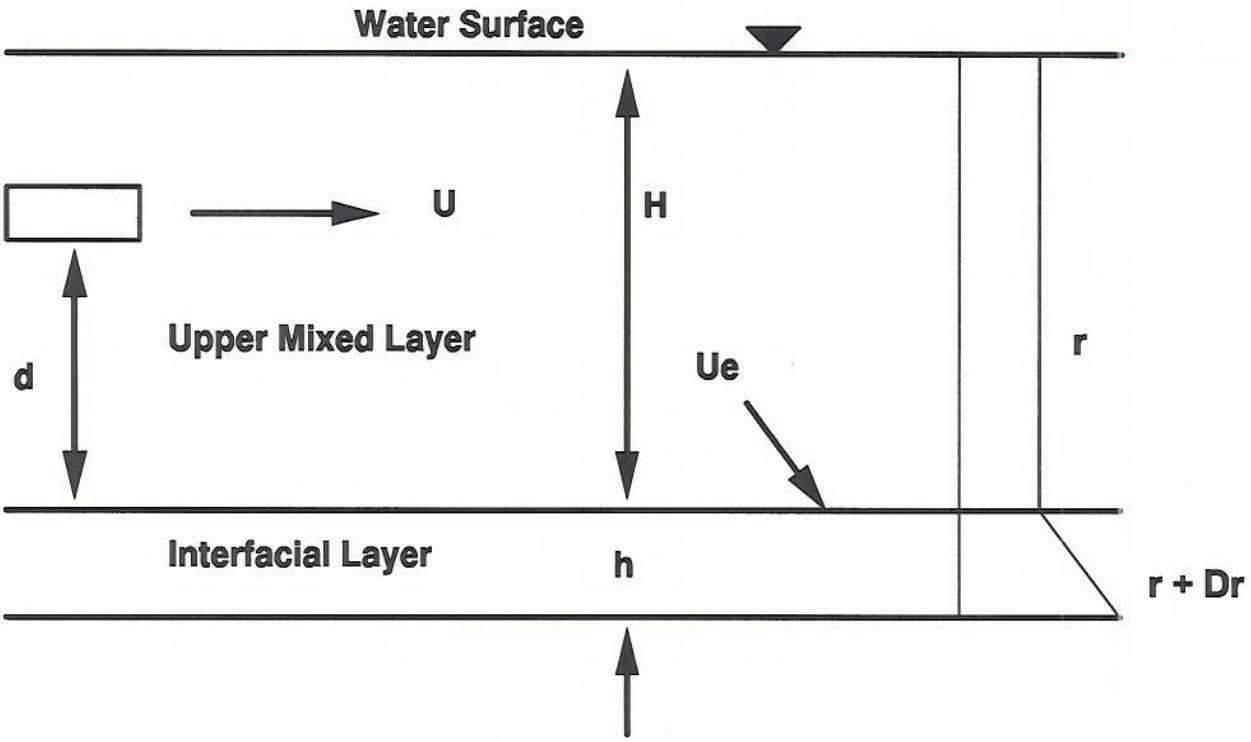

Figure 13 Definitions of Variables Used in the Formation of Entrainment Correlations

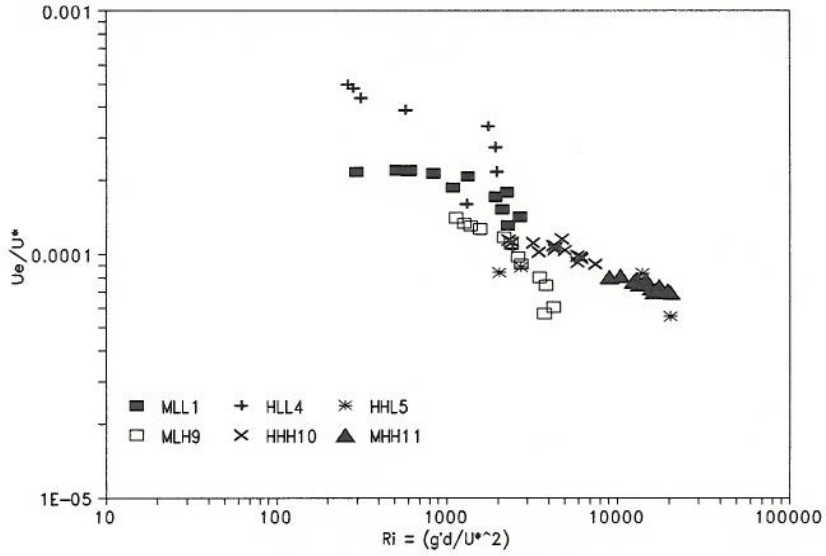

Figure 14 Entrainment Correlation Based on U*.

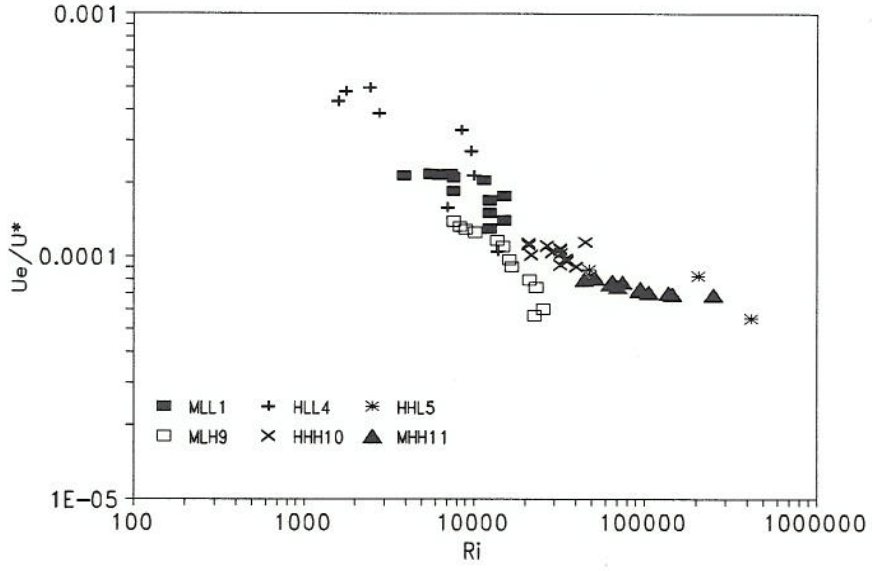

Figure 15 Entrainment Correlation Based on Combined Richardson Number